Title: Coexistence of the social semantic effect and non-semantic effect in the default mode network

Authors: Guangyao Zhang[1,2], Jinyi Hung[3], and Nan Lin[1,2,*]

Author Affiliations:
1 CAS Key Laboratory of Behavioral Science, Institute of Psychology
2 Department of Psychology, University of Chinese Academy of Sciences
3 Department of Audiology and Speech Language Pathology, Mackay Medical College

Corresponding Author:
Nan Lin
E-mail address: linn@psych.ac.cn

Abstract

Neuroimaging studies have found both semantic and non-semantic effects in the default mode network (DMN), leading to an intense debate on the role of the DMN in semantic processes. Four different views have been proposed: 1) The general semantic view holds that the DMN contains several hub regions supporting general semantic processes; 2) the non-semantic view holds that the semantic effects observed in the DMN (especially the ventral angular gyrus) are confounded by difficulty and do not reflect semantic processing per se; 3) the multifunction view holds that the same areas in the DMN can support both semantic and non-semantic functions; and 4) the multisystem view holds that the DMN contains multiple subnetworks supporting different aspects of semantic processes separately. Using an fMRI experiment, we found that in one of the subnetworks of the DMN, called the social semantic network, all areas showed social semantic activation and difficulty-induced deactivation. The distributions of two non-semantic effects, that is, difficulty-induced and task-induced deactivations, showed dissociation in the DMN. In the bilateral angular gyri, the ventral subdivisions showed social semantic activation independent of difficulty while the dorsal subdivisions showed no semantic effect but difficulty-induced activation. Our findings provide two insights into the semantic and non-semantic functions of the DMN, which are consistent with both the multisystem and multifunction views: First, the same areas of the DMN can support both social semantic and non-semantic functions; second, similar to the multiple semantic effects of the DMN, the non-semantic effects also vary across its subsystems.

Keywords

Default mode network; Angular gyrus; Social semantic processing; Difficulty; Working memory load; Narrative

Introduction

Semantic processing refers to the processing of meanings. It is central to many cognitive functions, such as language, reasoning, and problem-solving. Many neuroimaging studies have investigated brain activation during semantic processing. An important finding is that the brain areas activated during semantic processing largely overlap with the default mode network (DMN), a brain network that is characterized by high activity when individuals are left to think to themselves undisturbedly (Binder et al. 2009; Raichle et al. 2001; Smallwood et al. 2021; Wang et al. 2021). To explain the overlap between the DMN and the semantic network, Binder et al. (1999) proposed that semantic processing constitutes a large component of the cognitive activity occurring during the resting state. They examined this hypothesis by comparing brain activity during a resting state, a perceptual task, and a semantic retrieval task in an fMRI experiment. The DMN showed higher activation during the resting state than during the perceptual task but equal activation during the resting and semantic conditions, which is consistent with their hypothesis. Binder and Desai (2011) further proposed a neurobiological model of semantic processing, which assumes that the DMN contains several hub regions that combine semantic knowledge distributed in the sensory, motor, and emotional systems and supports general semantic processes. We refer to this view as the general semantic view of the DMN.

However, some later studies have indicated that the observed semantic effect in the DMN could be confounded by task difficulty. The core evidence of these studies comprises two domain-general effects observed in the DMN, which are difficulty-induced deactivation (difficult < easy) and task-induced deactivation (task < rest). In an fMRI study, Humphreys et al. (2015) investigated brain activation in several semantic and non-semantic tasks. They found that the core regions of the DMN, including the ventral angular gyrus (AG), posterior cingulate (PC), and medial frontal cortex, showed a task-induced deactivation effect (rest > task) in not only nonsemantic tasks but also semantic ones. Humphreys et al. (2015) interpreted this finding as that when a neural region is not critical to task function it is deactivated. The same interpretation has been used to explain some well-known phenomenon, for example, the deactivation of auditory areas during visual processing. Humphreys et al. (2015) argued that this interpretation is consistent with the "limited-capacity" model of neural processing (Handy, 2000) and the hypothesis that there are online plasticity mechanisms to balance metabolic energy consumption against task performance (Attwell & Laughlin, 2001). Humphreys et al. (2015) paid special attention to the ventral AG, which is viewed as a hub region of the semantic network by many researchers (Binder et al., 2009; Bonner et al., 2013; Lin et al., 2018a; Seghier, 2010). They found a negative correlation between ventral AG activation and reaction time (RT), indicating that activation of the ventral AG is sensitive to task difficulty. In a later study, Humphreys and Lambon Ralph (2017) further examined the difficulty effect in the DMN using a semantic task and a visuospatial task. They found a difficulty-induced deactivation effect (difficult < easy) in the ventral AG, PC, and medial frontal cortex in both tasks but found no semantic effect in these regions. Therefore, they proposed that the ventral AG is an automatic bottom-up domain-general buffer of active information, whose function is suppressed when tasks demand executive inputs from the frontoparietal network (Humphreys et al. 2021). More striking evidence has been reported by Graves et al. (2017). They found that the typical greater brain activation pattern to words than non-words during lexical decision, mainly overlapped with the DMN and often explained as the lexical semantic effect, can be flipped by using low-frequency words that are

more difficult to process than those typically used. Therefore, the activation of the DMN during lexical decision mainly reflects the difficulty effect rather than the semantic effect. Taken together, these observations lead to the non-semantic view of the DMN (Humphreys et al. 2015; 2021; Jackson et al. 2019), which holds that the semantic effects observed in most DMN regions are confounded by task difficulty and do not reflect semantic processing per se.

Mattheiss et al. (2018) investigated the semantic and non-semantic effects in the DMN using an fMRI experiment and proposed a third view for the DMN, which we refer to as the multifunction view of the DMN. In their experiment, Mattheiss et al. (2018) asked participants to perform a lexical decision task, in which the imageability of the word stimuli was manipulated. They replicated the finding of Graves et al. (2017) that the DMN showed a stronger activation to non-words than words. Using a multivariate analysis, they further found that most of the areas that showed a stronger activation to non-words than words in the study by Graves et al. (2017) contained sufficient information to distinguish high- from low-imageability words. Because the RT and accuracy were matched between the high- and low-imageability conditions, Mattheiss et al. (2018) proposed that the classification of high- and low-imageability words relied on semantic representation. Combining the difficulty effect reflected by the univariate results and the semantic effect reflected by the multivariate results, they concluded that the same areas in the DMN can support both semantic and non-semantic functions.

The last view regarding the function of the DMN in semantic processes holds that the DMN consists of multiple subnetworks that support different aspects of semantic processes separately (Huth et al. 2016; Lin et al. 2020). We refer to this view as the multisystem view of the DMN. Using a data-driven approach, Huth et al. (2016) modeled the impact of multiple semantic features on participants' brain activation while listening to narrative stories. They identified a semantic network whose activation could be reliably predicted by semantic features while listening to new stories. This semantic network consists mostly of areas of the DMN. Further analysis showed that most areas within the semantic network represent information about specific semantic domains or knowledge types, forming an intricate semantic atlas. Several distinct semantic areas were found in and around the AG, with some areas being selective for social concepts, while others were selective for numeric, visual, or tactile concepts. Similarly, Tamir et al. (2016) found functional dissociation within the DMN when reading fiction. Using fMRI, they found that the dorsal medial prefrontal cortex (DMPFC) subnetwork of the DMN responded preferentially to passages with social content, while the medial temporal lobe (MTL) subnetwork of the DMN responded preferentially to vivid passages. Two latter fMRI studies have demonstrated functional dissociation within the DMN using simpler and more controlled experimental tasks. Lin et al. (2018a) investigated the brain activations evoked by social and sensory-motor semantic information by manipulating the sociality and imageability of words in a word comprehension task. They found functional dissociation between DMN regions, with some regions being sensitive to the social meaning of words and some other regions being sensitive to the sensory-motor meaning of words. Later, using a semantic plausibility judgment task, Lin et al. (2020) further found that another set of regions, which also overlaps with the DMN, is sensitive to the semantic plausibility of phrases. Again, the AG and its surrounding areas showed complex functional dissociation, with the anterior dorsal part being sensitive to semantic plausibility, the anterior ventral part being sensitive to social semantic processing, the posterior part being sensitive to sensory-motor semantic processing, and the middle ventral part being sensitive to both social and

sensory-motor semantic processing (Lin et al. 2020). In summary, these studies have collectively indicated that different parts of the DMN are sensitive to different aspects of semantic processing. Therefore, even if task difficulty can explain some of the previously observed semantic effects, it alone cannot explain all semantic effects that are associated with different parts of the DMN.

The relationship between semantic and non-semantic effects in the DMN remains unclear in several aspects. There is compelling evidence that the DMN contains multiple subnetworks that are sensitive to different aspects of semantic processing; however, it remains unclear whether and how each of the semantic subnetworks in the DMN is sensitive to non-semantic factors, such as task difficulty. It is also unclear whether specific types of semantic processing can selectively determine the polarity of the task effect (i.e., task-induced activation/deactivation) in each of these semantic subnetworks, which has been viewed as an important indicator of functional selectivity for semantic processing (Humphreys et al. 2015; 2021; Jackson et al. 2019).

The relationship between difficulty-induced deactivation and task-induced deactivation in the DMN, both considered as non-semantic effects, is also unclear. These two effects together formed the main evidence for the non-semantic view of the DMN; especially, in the ventral AG, they have both been interpreted according to automatic bottom-up buffering processes (Humphreys et al. 2015; 2021). However, although task-induced deactivation in the DMN has been robustly found across many tasks (Humphreys et al. 2015), it remains unclear whether difficulty-induced deactivation in the DMN is stable across multiple tasks. Using five fMRI experiments with 252 participants in total, Yarkoni et al. (2009) investigated the relationship between trial-by-trial differences in the RT and brain activation. A positive correlation between the RT and activation being consistent across experiments was observed in extensive brain regions in the task-positive network (TPN; Fox et al., 2005); however, no gray matter region showed a consistent negative correlation between the RT and activation across experiments. In addition, a recent study indicated that the two types of deactivation may have different distributions in the DMN. Using an fMRI experiment, Meyer and Collier (2020) investigated the effect of difficulty in social and non-social working memory tasks. The difficulty-induced deactivation effect was found only in the non-social working memory task and only in the DMPFC subnetwork of the DMN. Regarding the task effect, they found that the DMPFC subnetwork showed task-induced activation rather than deactivation, while the MTL and core subnetworks showed task-induced deactivation.

One way to clarify the relationships between the multiple semantic effects and non-semantic effects in the DMN is to investigate the semantic processes with distinctive neural correlates separately. Therefore, our study focused on social semantic processing, that is, the processing of meanings about the interaction or interrelationships between individuals. Brain activation associated with social semantic processing has been consistently found in a subset of DMN areas, using univariate analyses (Zhang et al. 2021; Arioli et al. 2021; Binney et al. 2016; Lin et al. 2015; 2018a; 2018b; 2019; 2020; Zahn et al. 2007) and multivariate analyses (Thornton and Mitchell 2018). These areas include the bilateral anterior temporal lobe (ATL), temporoparietal junction (TPJ; overlapping with the ventral AG), DMPFC, and PC/precuneus, which are collectively referred to as the social semantic network (Lin et al. 2020; Zhang et al. 2021). We aimed to investigate the following three questions: First, can the social semantic effect and the difficulty effect collocate in the same areas of the DMN? Second, is the polarity of the task effect in the social semantic network selectively determined by social semantic processing? Third, do difficulty-induced deactivation and task-induced deactivation share the same neural correlates

during social semantic processing?

To answer these questions, we conducted an fMRI experiment in which social semantic processing and task difficulty were manipulated. The neural correlates of the social semantic effect, difficulty effect (difficulty-induced activation and deactivation), and task effect (task-induced activation and deactivation) were examined together in this experiment. In addition, to examine the relationship between social semantic processing and the polarity of the task effect across multiple experimental tasks and stimuli, we also examined the results of five previous studies of social semantic processing (Lin et al. 2018a; 2018b; 2019; 2020; Zhang et al. 2021).

Among the brain areas in the DMN, we paid special attention to the AG because its function in semantic and nonsemantic processing is under an intense debate as introduced above. The AG is one of the core areas of the DMN, locating at the posterior part of the inferior parietal lobule. It is one of the major connector hubs linking different subsystems of the brain, having rich connectivities with the sensory and motor association areas as well as the multimodal areas in the frontal, parietal, and temporal lobes (Bonner et al., 2013; Seghier, 2013; Uddin et al., 2010). The function of the AG is associated with a variety of cognitive domains, including language comprehension, episodic memory, mathematical processing, spatial cognition, and social cognition (Seghier, 2013; Cabeza et al., 2012). During semantic processing, the AG has been found to be related with representing social, sensory-motor, and event concepts (Binder and Desai, 2011; Lin et al., 2018a), integrating elementary conceptual attributes represented in the modality-specific association cortices (Bonner et al., 2013; Fernandino et al., 2016), combining the word meanings in a phrase (Graessner et al., 2021; Price et al., 2015), integrating the word meanings in a sentence (Humphries et al., 2006; Pallier et al., 2011), and integrating the context and target information in a narrative (Branzi et al., 2021). Importantly, the AG is a structurally and functionally heterogeneous region (Caspers et al., 2006; Seghier, 2013; Seghier et al., 2010; Uddin et al., 2010), which can at least partially account for its functional complexity. For example, Wilson-Mendenhall et al. (2013) found that the ventral AG is sensitive to mentalizing and concepts associated with social interaction while the dorsal AG is sensitive to numerical cognition and concepts associated with arithmetic. On the other hand, it has also been found that the dorsal AG shows a greater response when difficulty is increased, whereas ventral AG shows the inverse pattern (Humphreys and Lambon Ralph 2017; Humphreys et al., 2021). Previous studies on the relationship between the semantic and difficulty effects have focused on general or sensory-motor semantic processing rather than social semantic processing (Humphreys et al. 2015; Humphreys & Lambon Ralph 2017; Mattheiss et al. 2018) and it has been found that the neural correlates of these semantic effects differ from those of social semantic processing in the AG (Lin et al. 2018a). Therefore, examining the relationship between the social semantic effect and difficulty effect in the AG can provide a new and important aspect of evidence on the roles of the subdivisions of the AG in semantic and non-semantic processes.

Methods

Participants

In total, 24 healthy undergraduate and graduate students (14 women) participated in our fMRI experiment. The mean age of the participants was 21.7 years (SD = 2.6 years). All the participants were right-handed and native Chinese speakers. None of them had experienced psychiatric or neurological disorders or had sustained a head injury. Before the study began, all protocols and procedures were approved by the Institutional Review Board of the Magnetic

Resonance Imaging Research Center of the Institute of Psychology of the Chinese Academy of Sciences. Each participant read and signed the informed consent form before the experiment.

Design and materials

In the fMRI experiment, we manipulated the social semantic richness (high/low) of the stimuli and the difficulty (high working memory load/low working memory load) of the tasks, resulting in four conditions [high social semantic richness and high working memory load (HSHL); high social semantic richness and low working memory load (HSLL); low social semantic richness and high working memory load (LSHL); and low social semantic richness and low working memory load (LSLL)].

The experimental materials were 32 high social-semantic-richness and 32 low social-semantic-richness narratives, with each narrative consisting of four sentences. All of the narratives were used in a previous study (Zhang et al. 2021), in which we detailed how the social semantic richness and control variables of the narratives were manipulated and controlled. In brief, each narrative contains a protagonist whose name was "刘梅" or "李军." The high social-semantic-richness narratives were always about the social interactions between the protagonist and other characters, while the low social-semantic-richness narratives contained no social interaction. To confirm our manipulation of social semantic richness, we obtained the social semantic richness scores of the materials at both the narrative and sentence levels using two rating experiments (each recruiting 16 participants). The narrative- and sentence-level social semantic richness scores of the high social-semantic-richness narratives were both significantly higher than those of the low social-semantic-richness narratives (Table 1). In addition, we carefully matched a series of variables between the high and low social-semantic-richness narratives, which included the sentence- and narrative-level semantic plausibilities; coherence of narratives; number of words per narrative and per sentence; number of characters per narrative, per sentence, and per word; and word frequency (Table 1).

We used an n-back task to manipulate the task difficulty in the fMRI experiment. To this end, the stimuli were grouped into 16 high social-semantic-richness blocks and 16 low social-semantic-richness blocks, each of which contained two narratives. The two narratives of the same block always shared the same name of the protagonist and were presented sentence by sentence in an interlaced manner: The first two sentences were the starting sentences of the two narratives, and the remaining sentences were presented in a pseudorandom order, following one of four predefined structures (Table S1). In each block, the participants read the stimuli and made judgments by pressing buttons from the third sentence to the last sentence. In the easy condition, the participants were asked to judge whether the current sentence was of the same narrative as the preceding sentence (one-back task); in the difficult condition, the participants were asked to judge whether the current sentence was of the same narrative as the second preceding sentence (two-back task).

The n-back task used in this study had two advantages. First, identical stimuli can be used in both easy and difficult conditions, avoiding potential confounding between difficulty and stimulus-related differences. In previous studies of the semantic and difficulty effects, easy and difficult semantic conditions were often associated with different types of stimuli (e.g., unambiguous words vs. ambiguous words). These stimuli differ not only in processing difficulty but also in semantic content and semantic richness. In our task, manipulation of difficulty was independent of the stimuli. The participants needed to encode the meaning of every sentence they

see and maintain the meaning of all sentences in their mind until the end of the block, regardless of the one-back task or the two-back task. Second, the n-back paradigm is a classic method for manipulating task difficulty. Therefore, our results can be easily compared with the findings of a large body of literature on task difficulty.

To ensure that the n-back task could be successfully performed, we conducted a rating experiment and two preliminary behavioral experiments before the fMRI experiment, each of which recruited 16 participants who did not participate in the fMRI experiment. In the rating experiment, we investigated the coherence of the sentence pairs to be judged in the fMRI task. The participants were asked to rate the extent to which the meanings of each pair of sentences were connected using 7-point scales (7 = very high and 1 = very low). As shown in Table S2, the within-narrative sentence pairs had much higher coherence scores than the between-narrative sentence pairs in all four experimental conditions, indicating that participants could successfully perceive the connection between the within-narrative sentence pairs and the disconnection between the between-narrative sentence pairs. We then conducted the first preliminary behavioral experiment to examine whether the contents of our stimuli can support correct responses in the n-back task. In contrast to the fMRI task, this preliminary experiment was conducted such that the stimuli of each block were presented in an accumulative manner, that is, during the presentation of the current sentence, while all of its preceding sentences of the same block could still be seen. The participants were asked to respond as accurately as possible without any time limit. As a result, all conditions yielded a high accuracy [mean (SD) accuracies: 97.7% (2.4%) for HSHL, 96.6% (4.8%) for HSLL, 97.8% (4.3%) for LSHL, 98.3% (2.2%) for LSLL]. We then conducted a second preliminary behavioral experiment to examine the impact of working memory load on the task and to evaluate the appropriate presentation time of the sentences for the fMRI task. To this end, a sentence would not disappear until the participants pressed a button. They were asked to respond as rapidly and accurately as possible. The results are presented in Table S3. The mean accuracies for all conditions were higher than 90%. The working memory load significantly affected the accuracy ($z = 7.625$, $p < .001$) and RT ($t = 32.825$, $p < .001$). The social semantic effect and its interaction with the working memory load were non-significant (social semantic effect on accuracy, $z = 0.125$, $p = .900$; social semantic effect on the RT, $t = 1.447$, $p = .158$; interaction effect on accuracy, $z = 1.082$, $p = .279$; interaction effect on the RT, $t = 1.162$, $p = .245$). According to the RT data of this preliminary experiment, we set the presentation time of the sentences to 5 s in the fMRI experiment, which was approximately 2 SD over the mean RT of the difficult (two-back) conditions.

The fMRI experiment consisted of four runs of 7 min and 6 s each. Each run included eight blocks, two for each condition. In the first 10 s of each run, the participants were shown a fixation. At the start of each block, a cue ("#1-back#" or "#2-back#") was presented for 2 s to indicate the task requirements. The participants then read the eight sentences of each block sequentially. Each sentence was presented for 5 s, and from the third sentence to the last sentence of each block, they were asked to make a judgment by pressing buttons. The interblock intervals had a fixed duration of 10 s. All narratives were presented only once for each participant in either one- or two-back condition. The correspondence between the blocks and conditions and the order of the blocks were counterbalanced across runs and participants.

Image acquisition and preprocessing

Structural and functional data were collected using a GE Discovery MR750 3 T scanner at

the Magnetic Resonance Imaging Research Center of the Institute of Psychology of the Chinese Academy of Sciences. T1-weighted structural images were obtained using a spoiled gradient-recalled pulse sequence in 176 sagittal slices with 1.0-mm isotropic voxels. Functional blood-oxygenation-level-dependent data were collected using a gradient-echo echo-planar imaging sequence in 42 near-axial slices with 3.0-mm isotropic voxels (matrix size = 64 × 64; repetition time = 2000 ms; echo time = 30 ms).

The fMRI data were preprocessed using the Statistical Parametric Mapping software (SPM12; http://www.fil.ion.ucl.ac.uk/spm/) and DPABI V3.0 (Yan et al. 2016). For the preprocessing of the task fMRI data, the first five volumes of each functional run were discarded to reach signal equilibrium. Slice timing and 3-D head motion correction were performed. Subsequently, a mean functional image was obtained for each participant, and the structural image of each participant was coregistered to the mean functional image. Thereafter, the structural image was segmented using a unified segmentation module (Ashburner and Friston 2005). Next, a custom, study-specific template was generated by applying diffeomorphic anatomical registration through exponentiated lie algebra (Ashburner 2007). The parameters obtained during segmentation were used to normalize the functional images of each participant into the Montreal Neurological Institute space by applying the deformation field estimated by segmentation. The functional images were subsequently spatially smoothed using a 6-mm full-width-half-maximum Gaussian kernel.

Data analysis

Behavioral data analyses

For each participant and each condition, we removed the RT measures that either corresponded to incorrect responses or were 3 SDs from the mean of the corresponding subset. To analyze the RTs, we fitted a linear mixed model to raw RT data using the lme4 package in R. The model included fixed effects for social semantic richness (high, low), working memory load (high, low), and an interaction item (social semantic richness by working memory load). For the random effects, the participant, block, and position of the sentence in each block were included as random factors. Because including any random slope could lead to convergence failures, the model was built with only a random intercept. For each of the three fixed effects, its statistical significance was assessed using the Satterthwaite approximation for degrees of freedom from the lmerTest *R* package (Kuznetsova et al. 2017), and we reported the corresponding *t*-values and *p*-values. For accuracy, we fitted a generalized linear mixed model with a binary distribution. For the fixed and random effects, the model was built in the same manner as in the analysis of the RTs. In the statistical analyses, we reported the *z*-values and corresponding *p*-values for each of the fixed effects.

FMRI data analyses

Whole-brain analysis

Statistical analyses of the task fMRI data were conducted according to two-level, mixed-effects models implemented in SPM12. Because brain activation during the processing of a narrative can vary considerably (Lin et al. 2018b; Xu et al. 2005), we modeled the BOLD signals of the stimuli sentence by sentence. Therefore, at the first level, a generalized linear model was built by including 32 covariates of interest, corresponding to the eight sentences of each block for the four experimental conditions. The six head motion parameters obtained via head motion correction were included as nuisance regressors. A high-pass filter (128 s) was used to remove

low-frequency signal drift. After the estimation of the model parameters, participant-specific statistical maps were generated. Since the participants only needed to respond to the last six sentences of each block, we only focused on the last six covariates of each condition. The beta maps of the last six covariates of each condition were averaged into a mean beta-map, resulting in a single beta-map for each condition. These participant-specific statistical maps were then entered into a second-level random-effects analysis, in which a flexible factorial design was applied to accommodate a 2 × 2 within-subject design. The social semantic activation effect and difficulty effect, as well as their interaction, were examined. Multiple comparison corrections of the whole-brain analysis results were conducted using cluster-level FWE correction ($p < .05$) as implemented in SPM12 (voxel-wise $p < .001$).

ROI analysis

Three sets of regions of interest (ROIs) were defined for targeted analysis of our research questions. The first set of ROIs consisted of the component regions of the task-defined social semantic network (Fig. 1a). We used the ROIs identified by Lin et al. (2019). To localize the social semantic network, Lin et al. (2019) asked participants to perform a semantic relatedness judgment task on verb pairs. The verb pairs were either rich or poor in their social semantic information. The comparison between the high and low social-semantic-richness verb pairs revealed six clusters corresponding to the six classic component regions of the social semantic network. Each cluster was defined as an ROI. We used the ROIs obtained by Lin et al. (2019) for two reasons. First, Lin et al. (2019) localized the social semantic network using a classic semantic comprehension task (i.e., semantic relatedness judgment for word pairs), controlling for non-social semantic activation and the effects of several lexical semantic variables. Second, Lin et al. (2019) used the same MRI scanner, scanning parameters, and data analysis procedures used in our study, making the brain locations in the two studies highly comparable. In addition to the ROIs identified by Lin et al. (2019), we also used a Neurosynth-based social semantic network as a supplementary large-scale ROI to examine the robustness of our results in the social semantic network (Fig. S1a). Zhang et al. (2021) defined the social semantic network as the overlap between the results of two Neurosynth-based meta-analyses, using “social” and “semantic” as the key terms (and using the default settings of the Neurosynth: association test; false discovery rate criterion of 0.01). This method, as the authors argued, is based on two assumptions: First, social semantic processing is a fundamental cognitive component for most social cognitive tasks; second, social semantic representation is a basic type of semantic representation that should be activated in a considerable proportion of semantic studies. Zhang et al. (2021) found that this method revealed a set of brain regions that is highly similar to the finding of the well-controlled experimental studies on social semantic processing, which indicates that the social semantic network is located at the junction of the semantic and social networks, serving as a component of both of them. We used this method as a supplementary way to define the social semantic network because it was based on a very large dataset (1302 social studies and 1031 semantic studies), which can better indicate the generalizability of our finding to the research on social cognition and semantic processing. Note that the original network defined by Zhang et al. (2021) contains a few unconnected voxels and we retained only the clusters that contain more than 10 voxels in the ROI.

The second set of ROIs consisted of the functional subdivisions of the bilateral AG (Fig. 1b). We defined the AG by merging the AG areas of two frequently used atlases, that is, the AAL and Harvard–Oxford atlases. We then conducted a Neurosynth-based functional parcellation analysis

of the AG (de la Vega et al. 2018; Hung et al. 2020). A coactivation matrix between each voxel in the bilateral AG and that in the rest of the brain was obtained using the Neurosynth database and was then applied with k-means clustering to group the AG into 2–10 clusters. The ideal number of clusters was selected on the basis of the highest silhouette score (Fig. S2), resulting in two functional subdivisions along the dorsal-ventral axis for the bilateral AG. In addition, because the silhouette score of the 4-cluster parcellation was higher than the scores of the 3- and 5-cluster parcellations, we also used the 4-cluster parcellation of the AG as a set of supplementary ROIs to inspect the result patterns. This supplementary parcellation separates the dorsal AG into a mediodorsal cluster and a laterodorsal cluster, and the ventral AG into a dorsoventral cluster and a ventroventral cluster (Fig. S1b). For both the 2- and 4-cluster parcellations of the bilateral AG, we separated each of the bilaterally distributed clusters into left and right parts, resulting in four and eight ROIs, respectively.

The last set of ROIs consisted of the three resting-state subnetworks of the DMN (Fig. 1c), named the core subnetwork, DMPFC subnetwork, and MTL subnetwork (Andrews-Hanna et al. 2010; Yeo et al. 2011). Previous studies have indicated that the cortical distributions of the social semantic, difficulty, and task effects are all associated with resting-state functional organizations in the brain (Humphreys & Lambon Ralph 2017; Lin et al. 2018a; Meyer and Collier 2020; Smallwood et al. 2021; Tamir et al. 2016). Therefore, exploring the result patterns in the resting-state subnetworks of the DMN can help us to further understand how these effects are distributed in the DMN. We defined this set of ROIs based on the 17 resting-state networks identified by Yeo et al. (2011).

As in the whole-brain analysis, the ROI analysis of the experimental data of our study also focused on the third to eighth covariates of each condition. The voxel-based beta values of each covariate obtained in the first-level analysis were averaged for each ROI. For each ROI, we fitted a linear mixed model to the beta values of the ROI using the lme4 package in R. The model included four fixed effects: three fixed slopes for social semantic richness (high/low) and difficulty (high working memory load/low working memory load) and their interaction (social semantic richness by working memory load) and a fixed intercept for the task effect. The participant and the position of the sentence in the block were included as random factors. Because including any random slope could lead to convergence failures, the model was built with only a random intercept. For each of the four fixed effects, we assessed its statistical significance using the Satterthwaite approximation for degrees of freedom from the lmerTest *R* package (Kuznetsova et al. 2017) and reported corresponding *b*-values, SE, and *t*-values.

We further inspected the data of five previous studies (Lin et al. 2018a; 2018b; 2019; 2020; Zhang et al. 2021) in the same sets of ROIs. An overview of these studies is shown in Table 2. The data acquisition parameters and preprocessing procedures of these studies were the same as those used in our study. For all five studies, we set the high and low social-semantic-richness conditions of the original designs as the target and control conditions, respectively, and examined the social semantic effect using a paired t-test and the polarity of the task effect in both high and low social-semantic-richness conditions using a one-sample t-test.

For all of the results of the ROI analysis, we conducted Bonferroni correction to adjust multiple comparisons in each set of ROIs (e.g. the six ROIs of the social semantic network), in which the significance level is divided by the number of ROIs.

Results

Behavioral results

Across the four conditions, the mean (SD) RT was 1834 (391) ms. For each condition, the mean (SD) RTs were 1992 (427) ms for HSHL, 1726 (325) ms for HSLL, 1926 (349) ms for LSHL, and 1691 (393) ms for LSLL. We found the main effect of difficulty (t = 13.239, df = 4087.780, p < .001), wherein the RT was shorter in the low working-memory-load condition. The main effect of social semantic richness was non-significant (t = - 1.160, df = 29.830, p = .255), and there was no interaction between social semantic richness and working memory load (t = - 0.551, df = 4086.700, p = .582).

The mean (SD) accuracy across the four conditions was 90.6% (9.01%). For each condition, the mean (SD) accuracies were 87.6% (9.4%) for HSHL, 93.7% (8.2%) for HSLL, 88.3% (9.4%) for LSHL, and 93.1% (7.9%) for LSLL. We found the main effect of difficulty (z = - 6.46, p < .001), wherein the participants responded with a higher accuracy for the low working-memory-load condition. The main effect of social semantic richness was not significant (z = - 0.16, p = .874), and there was no interaction between social semantic richness and working memory load (z = 0.82, p = .413).

FMRI results

Whole-brain analysis results

The results of the whole-brain analysis are shown in Fig. 2 and Table 3. Social semantic activation (high social semantic richness > low social semantic richness) was found in the bilateral temporal lobe, extending from the ATL to the TPJ, DMPFC, PC, left orbitofrontal cortex, and ventromedial prefrontal cortex. A reversed social semantic effect (low > high) was found in the bilateral frontal pole and left orbitofrontal cortex. These results coincide with the findings of previous studies of social semantic processing (Contreras et al. 2012; Lin et al. 2018b; Zhang et al. 2021).

Difficulty-induced activation (high working memory load > low working memory load) was found in the frontoparietal multiple demand network (Duncan 2010), reflecting the classic finding of the working memory load effect. However, difficulty-induced deactivation was only found in a few brain regions, including the postcentral lobe, PC, right occipital pole, and right supramarginal gyrus. No overlap or interaction was found between the social semantic richness and difficutlty effects in the whole-brain analysis.

Task-induced activation and deactivation, mainly distributed in the TPN and DMN, respectively, were in agreement with the classic finding of the task effect. Task-induced activation was also observed in the left lateral temporal cortex. Notably, we did not find task-induced deactivation in the AG, as in some previous studies (e.g., Humphreys et al., 2015).

ROI analysis results

Can the social semantic effect and difficulty effect collocate in the same areas of the DMN?

To answer this question, we analyzed the social semantic and difficulty effects and their interaction in the ROIs of the social semantic network and in the functional subdivisions of the bilateral AG.

In the social semantic network, all ROIs showed social semantic activation and difficulty-induced deactivation (Table 4). No ROI showed an interaction between social semantic

richness and difficulty. We further inspected the homogeneity of the result patterns within each ROI. The result patterns for both social and difficulty effects were highly homogeneous within each ROI (Fig. S3). The results using the Neurosynth-based social semantic network reflected the same pattern (Table S4). These results indicate that independent social semantic activation and difficulty-induced deactivation reliably coexist in the entire social semantic network and together modulate its activation.

For the Neurosynth-based functional subdivisions of the AG, when using the 2-cluster parcellation, the bilateral dorsal AG showed a strong difficulty-induced activation (difficult > easy; Table 4), which coincides with the findings of previous studies (Humphreys & Lambon Ralph 2017); meanwhile, the bilateral ventral AG, which partially overlaps with the TPJ regions of the social semantic network, showed a strong social semantic activation (high social semantic richness > low social semantic richness; Table 4). When using the 4-cluster parcellation, we found basically the same results as when using the 2-cluster parcellation: both the mediodorsal and laterodorsal AG showed a strong difficulty-induced activation; both the dorsoventral and ventroventral AG showed a strong social semantic activation (Table S4). An additional finding is that when the ventral AG is separated into more fine-gained functional subdivisions, the subdivisions showed sensitivity to task difficulty: the bilateral dorsoventral AG showed difficulty-induced activation while the right ventroventral AG showed difficulty-induced deactivation (Table S4). Again, we did not find any interaction effect between social semantic processing and difficulty in any ROI. Therefore, the social semantic activation observed in the AG was also independent of the difficulty effect, and it coexisted with difficulty-induced activation as well as difficulty-induced deactivation in the fine-gained functional subdivisions of the ventral AG.

Is the polarity of the task effect in the social semantic network selectively determined by social semantic processing?

To answer this question, we inspected the results of our study and five previous studies that included high and low social-semantic-richness conditions. In total, 12 independent contrasts between high and low social-semantic-richness conditions using different types of stimuli (e.g., verbs, nouns, phrases, word lists, sentences, and narratives) were included, resulting in 72 independent data points (12 contrasts × 6 ROIs of the social semantic network).

We first inspected the social semantic effect (high > low) in each contrast and ROI. As shown in Fig. 3, significant social semantic effects were observed in all contrasts in the left ATL (LATL); in 11 of the 12 contrasts in the right ATL, left DMPFC (LDMPFC), and left TPJ; in 10 of the 12 contrasts in the right TPJ; and in 8 of the 12 contrasts in the PC. In total, 63 of the 72 data points revealed the social semantic effect, with no data points showing a reverse effect or trend (high < low). These results indicate a strong impact of social semantic processing on the activation of target ROIs.

If social semantic processing selectively determines the polarity of the task effect in the social semantic network, then only the high social-semantic-richness condition should evoke significant positive activation in it. However, only 23 of the 72 data points fulfilled this pattern. As shown in Fig. 3, in addition to social semantic processing, the locations of the ROIs also seemed to have a strong impact on the polarity of the task effect. In the bilateral ATL, where most of the high social-semantic-richness conditions evoked a positive activation, the low social-semantic-richness conditions also evoked a significant positive activation in about half of

the data points; in contrast, neither the high social-semantic-richness conditions nor the low social-semantic-richness conditions evoked any significant positive activation in the PC. Another factor that seems to modulate the polarity of the task effect is the stimulus type. As shown in Fig. 3, the tasks using sentences or narratives as stimuli were more likely to yield positive task effects and less likely to yield negative task effects than those using words or phrases in the bilateral ATL and TPJ.

In summary, the polarity of the task effect in the social semantic network seems to be determined by multiple factors rather than by social semantic processing alone.

Do difficulty-induced deactivation and task-induced deactivation share the same neural correlates during social semantic processing?

To answer this question, we compared the neural correlates of difficulty-induced deactivation and task-induced deactivation across the ROIs of the social semantic network, across the functional subdivisions of the AG, and across the three resting-state subnetworks of the DMN.

In the social semantic network, although all ROIs showed significant difficulty-induced deactivation, only two of them (LDMPFC and PC) showed significant task-induced deactivation, and the LATL showed a reverse pattern, that is, significant task-induced activation (Table 4). For the Neurosynth-based functional subdivisions of the AG, when using the 2-cluster parcellation, we found neither type of deactivation effect (Table 4); when using the 4-cluster parcellation, we found the right dorsoventral AG showing task-induced deactivation (but together with difficulty-induced activation) and the right ventroventral AG showing difficulty-induced deactivation (Table S4).

Among the three resting-state subnetworks of the DMN, task-induced deactivation was found in the core and MTL subnetworks, while difficulty-induced deactivation was found in the DMPFC subnetwork. To further inspect the task effect in the three subnetworks of the DMN, we analyzed the task effect in the five previous studies of social semantic processing (Fig. S4). The most stable task-induced deactivation effect was observed in the core subnetwork (significant in 10 of the 12 high social-semantic-richness conditions and in 11 of the 12 low social-semantic-richness conditions). The MTL subnetwork also showed a task-induced deactivation effect in most of the data points but occasionally showed the reverse pattern (task-induced activation). The DMPFC subnetwork, which showed the most robust social semantic activation among the three subnetworks, did not show significant task-induced deactivation in any study, even for the low social-semantic-richness conditions. It showed a significant positive task effect in 8 of the 12 high social-semantic-richness conditions and in 4 of the 12 low social-semantic-richness conditions.

In summary, the results of the ROI analysis indicate that although the neural correlates of difficulty-induced deactivation and task-induced deactivation overlap in some parts of the DMN (e.g., LDMPFC and PC), they still have considerable dissociation, especially across the three resting-state subnetworks: Difficulty-induced deactivation was mainly found in the DMPFC subnetwork while task-induced deactivation was mainly found in the core and MTL subnetworks.

Discussion

To investigate the social semantic and non-semantic effects in the DMN, we conducted an fMRI experiment in which we manipulated both social semantic processes and task difficulty. Several interesting findings were obtained. First, in a subnetwork of the DMN, called the social semantic network, all areas showed independent social semantic activation and difficulty-induced

deactivation. Second, the distribution of difficulty-induced deactivation and task-induced deactivation showed considerable dissociation in the DMN, especially across the three resting-state subnetworks of the DMN. Third, in the bilateral angular gyri, the ventral subdivisions showed social semantic activation independent of difficulty while the dorsal subdivisions showed no semantic effect but difficulty-induced activation. Taken together, these findings provide two insights into the semantic and non-semantic functions of the DMN: First, the same areas of the DMN can support both social semantic and non-semantic functions; second, similar to the multiple semantic effects of the DMN, non-semantic effects also vary across the subsystems of the DMN.

A novel and important finding of our study is the coexistence of the social semantic effect and difficulty effect in the same set of DMN areas, which provides new evidence for the multifunction view of the DMN. In comparison with the study by Mattheiss et al. (2018), our study expanded our knowledge of the multifunctional nature of the DMN from two new aspects. First, in comparison with the imageability effect studied by Mattheiss et al. (2018), the social semantic effect reflects a different aspect of semantic processes and is located in a different subnetwork of the DMN (Lin et al. 2018a; Tamir et al. 2016). Therefore, considering the findings of Mattheiss et al. (2018) and our study, the coexistence between the semantic and difficulty effects can occur in different types of semantic processes and in different subnetworks of the DMN. Second, Mattheiss et al. (2018) detected the semantic and difficulty effects using multivariate and univariate measurements, respectively; for the first time, our study demonstrated co-located semantic activation and difficulty-induced deactivation in the same areas of the DMN using the same univariate measurement.

Another important finding of this study is that two non-semantic effects, that is, difficulty-induced deactivation and task-induced deactivation, have considerable differences in their distributions, especially across the three resting-state subnetworks of the DMN. Difficulty-induced deactivation was mainly found in the DMPFC subnetwork; task-induced deactivation was mainly found in the core and MTL subnetworks. The dissociation of the two deactivation effects across the three resting-state subnetworks in our study is very similar to the findings of Meyer and Collier (2020), indicating that this dissociation is replicable. These results indicate that the two deactivation effects in the DMN have at least partially different functional locations and origins. They also indicate that the multisystem nature of the DMN modulates not only the organization of semantic functions in the DMN but also the organization of non-semantic functions.

Our results shed new light on the function of the AG in semantic and nonsemantic processes. We found independent social semantic and difficulty effects in the AG, both of which revealed a dorsal–ventral distinction. The ventral AG showed a strong social semantic effect, as found in several previous studies (Lin et al., 2018a; Lin et al., 2020; Wilson-Mendenhall et al., 2013; Zhang et al., 2021) while the dorsal AG did not show sensitivity to social semantic processing. The dorsal AG, which locates at the junction of the DMN and the multiple-demand network, showed difficulty-induced activation (difficult > easy) while the ventral AG as a whole (according to the 2-cluster parcellation) did not show sensitivity to task difficulty (Table 4). These dorsal–ventral differences in the AG are consistent with the previous finding that the ventral AG is mainly associated with social and language processing while the dorsal AG and its adjacent parietal areas are mainly associated with domain-general functions such as attention, working

memory, and executive control (Bzdok et al., 2016). The robust social semantic activation in the ventral AG can potentially provide a unified explanation for the engagement of this area in a variety of language and social cognitive tasks, such as sentence processing tasks, narrative comprehension tasks, false-belief reasoning tasks, and trait judgment tasks (Binder et al., 2009; Bzdok et al., 2016; Mar, 2011; Schurz et al., 2021), because the typical stimuli presented in these tasks are often rich in social semantic information. Interestingly, when separating the ventral AG into more fine-gained functional subdivisions, we found difficulty-induced activation in the dorsoventral AG and difficulty-induced deactivation in the ventroventral AG, which were both independent of the effect of social semantic processing (Table S4 and Fig. S3). Again, the results observed in the ventral AG are consistent with the multisystem and multifunction views of the DMN: The reverse difficulty effects in different subdivisions of the ventral AG indicate the multisystem nature of this area while the co-located and independent social-semantic and difficulty effects indicate the multifunctional nature of this area. In addition, the reverse difficulty effects observed in the dorsal and very ventral parts of the AG is also consistent with the view that different subdivisions of the AG are implicated in executive and automatic processing, respectively (Humphreys et al. 2015; Humphreys & Lambon Ralph 2017).

Our results also indicate that the polarity of the task effect in the social semantic network is determined by multiple factors, which is also consistent with the multifunction view of the DMN. Our results indicate that in addition to social semantic processing, the task effect in the social semantic network is also affected by the location and stimulus type. The location effect seems to be related to the task-irrelevant organizations of the DMN: The ATL and DMPFC, which are located within the DMPFC subnetwork, were more likely to show a positive activation than other areas; the PC, which is located in the core subnetwork, did not show a significant positive activation in any experiment (Fig. 3). The stimulus-type effect is related to the linguistic hierarchy of the stimuli. In comparison with words and phrases, sentences and narratives evoked more positive activations and fewer deactivations in the social semantic network (Fig. 3). This observation can be interpreted according to the view that the social semantic network supports not only semantic memory but also semantic accumulation during the comprehension of sentences and narratives (Zhang et al. 2021).

In addition, our study can be linked to previous studies on social working memory (Meyer and Collier 2020; Meyer et al. 2012; 2015), which investigated how the brain maintains and manipulates social information, such as the traits of familiar friends (Meyer et al. 2015; 2012) and the mental states of characters from a television show (Meyer and Collier, 2020) in working memory. As in our study, they manipulated both information types (social vs. non-social) and working memory loads. These studies found social effect (social > non-social) and difficulty-induced deactivation in the non-social conditions in the DMPFC subnetwork of the DMN, which is similar to our results. However, in contrast to our results, they found significant difficulty-induced activation (difficult > easy) in social conditions in the same areas. Based on such findings, Meyer and colleagues proposed that the DMPFC subnetwork uniquely supports social cognitive processes in working memory. There are at least two possible reasons why Meyer et al. and we observed reverse difficulty effects in high social conditions. First, the cognitive processes underlying memory load differ between studies. Meyer and colleagues manipulated memory loads by changing the number of items in the tasks. Therefore, in their studies, working memory loads were directly related to the amount of social information in working memory. In

our study, the participants were asked to judge the correspondence of the upcoming sentences to different narratives, thus they needed to remember the entire narratives both in the one-back task and in the two-back task. According to the current theories of narrative comprehension (e.g., theories in the study by Zwaan and Radvansky, 1998), this may be achieved by building two separate situation models for the two narratives and continuously updating both models using the input semantic information. In other words, in our task, the additional working memory load in the two-back task was associated with the memory of the correspondences of the sentences to the narratives rather than the amount of semantic information being remembered. Therefore, the working memory load in our study could be independent of the memory of semantic content per se. Second, unlike in our study, the social information studied by Meyer et al. is not lexical semantic knowledge. Rather, it is a specific type of personal semantic knowledge that has been referred to as the autobiographically significant knowledge, which may share more neural correlates with the episodic memory system than with the semantic system (Renoult et al. 2012). The impacts of these two differences on activation in the DMN will be explored in our future studies.

There were several limitations to our study. First, general semantic processes were controlled for in all critical comparisons of our study. Therefore, we have no evidence of or against the general semantic view of the DMN. Second, our study focused on the social semantic and difficulty effects and thus cannot indicate whether other types of semantic and non-semantic effects also coexist in the DMN. Third, the strength and distribution of difficulty-induced deactivation seem to be different from those in some previous studies (Graves et al. 2017; Humphreys & Lambon Ralph 2017). Therefore, the across-task consistency in the distribution of the difficulty effect should be investigated in the future.

In conclusion, we found the coexistence of social semantic and difficulty effects and the dissociation between difficulty-induced deactivation and task-induced deactivation in the DMN, supporting the multisystem and multifunction views of this network. Our findings indicate that the DMN has complex functional subdivisions, whose activity reflects the combination of multiple semantic and non-semantic effects. Future studies are warranted to compare the neural correlates of more types of semantic and non-semantic functions in the DMN to obtain a more comprehensive and systematic understanding of the multisystem and multifunctional nature of this network.

Acknowledgements This work was supported by National Natural Science Foundation of China (Grant numbers: 31871105) and by CAS Key Laboratory of Behavioral Science.

Declarations

***Funding*:** This study was funded by National Natural Science Foundation of China (Grant numbers: 31871105) and by CAS Key Laboratory of Behavioral Science.

***Conflict of interest*:** The authors declare that they have no conflict of interest.

***Availability of data and material*:** Data will be made available on reasonable requests for contacting the corresponding author.

***Code availability*:** Not applicable.

***Ethical approval*:** All procedures performed in studies involving human participants were in accordance with the ethical standards of the Institutional Review Board of the Magnetic Resonance Imaging Research Center of the Institute of Psychology of the Chinese Academy of

Sciences and with the 1964 Helsinki declaration and its later amendments or comparable ethical standards.

***Consent to participate*:** Written informed consent was obtained from all individual participants included in the study.

***Consent for publication*:** Written informed consent for publication was obtained from all individual participants included in the study.

Reference

Andrews-Hanna JR, Reidler JS, Sepulcre J, Poulin R, Buckner RL (2010) Functional-anatomic fractionation of the brain's default network. Neuron 65 (4):550–562. doi:10.1016/j.neuron.2010.02.005

Arioli M, Gianelli C, Canessa N (2021) Neural representation of social concepts: a coordinate-based meta-analysis of fMRI studies. Brain Imaging Behav 15 (4):1912–1921. doi:10.1007/s11682-020-00384-6

Ashburner J (2007) A fast diffeomorphic image registration algorithm. Neuroimage 38 (1):95–113. doi:10.1016/j.neuroimage.2007.07.007

Ashburner J, Friston KJ (2005) Unified segmentation. Neuroimage 26 (3):839–851. doi:10.1016/j.neuroimage.2005.02.018

Attwell D, Laughlin SB (2001) An Energy Budget for Signaling in the Grey Matter of the Brain. Journal of Cerebral Blood Flow & Metabolism 21 (10):1133–1145. doi:10.1097/00004647-200110000-00001

Binder JR, Desai RH (2011) The neurobiology of semantic memory. Trends Cogn Sci 15 (11):527–536. doi:10.1016/j.tics.2011.10.001

Binder JR, Desai RH, Graves WW, Conant LL (2009) Where is the semantic system? A critical review and meta-analysis of 120 functional neuroimaging studies. Cereb Cortex 19 (12):2767–2796. doi:10.1093/cercor/bhp055

Binder JR, Frost JA, Hammeke TA, Bellgowan PS, Rao SM, Cox RW (1999) Conceptual processing during the conscious resting state. A functional MRI study. J Cogn Neurosci 11 (1):80–95. doi:10.1162/089892999563265

Binney RJ, Hoffman P, Lambon Ralph MA (2016) Mapping the Multiple Graded Contributions of the Anterior Temporal Lobe Representational Hub to Abstract and Social Concepts: Evidence from Distortion-corrected fMRI. Cereb Cortex 26 (11):4227–4241. doi:10.1093/cercor/bhw260

Bonner MF, Peelle JE, Cook PA, Grossman M (2013) Heteromodal conceptual processing in the angular gyrus. NeuroImage 71:175–186. doi: 10.1016/j.neuroimage.2013.01.006

Branzi FM, Pobric G, Jung J, Lambon Ralph MA (2021) The Left Angular Gyrus Is Causally Involved in Context-dependent Integration and Associative Encoding during Narrative Reading. Journal of Cognitive Neuroscience 33 (6):1082–1095. doi:10.1162/jocn_a_01698

Bzdok D, Hartwigsen G, Reid A, Laird AR, Fox PT, Eickhoff SB (2016) Left inferior parietal lobe engagement in social cognition and language. Neuroscience & Biobehavioral Reviews 68:319–334. doi: 10.1016/j.neubiorev.2016.02.024

Cabeza R, Ciaramelli E, Moscovitch M (2012) Cognitive contributions of the ventral parietal cortex: an integrative theoretical account. Trends in Cognitive Sciences 16 (6):338–352. doi: 10.1016/j.tics.2012.04.008

Caspers S, Geyer S, Schleicher A, Mohlberg H, Amunts K, Zilles K (2006) The human inferior parietal cortex: Cytoarchitectonic parcellation and interindividual variability. NeuroImage 33 (2):430–448. doi: 10.1016/j.neuroimage.2006.06.054

Contreras JM, Banaji MR, Mitchell JP (2012) Dissociable neural correlates of stereotypes and other forms of semantic knowledge. Soc Cogn Affect Neurosci 7 (7):764–770. doi:10.1093/scan/nsr053

de la Vega A, Yarkoni T, Wager TD, Banich MT (2018) Large-scale Meta-analysis Suggests Low Regional Modularity in Lateral Frontal Cortex. Cereb Cortex 28 (10):3414–3428. doi:10.1093/cercor/bhx204

Duncan J (2010) The multiple-demand (MD) system of the primate brain: mental programs for intelligent behaviour. Trends Cogn Sci 14 (4):172–179. doi:10.1016/j.tics.2010.01.004

Fernandino L, Binder JR, Desai RH, Pendl SL, Humphries CJ, Gross WL, Conant LL, Seidenberg MS (2016) Concept Representation Reflects Multimodal Abstraction: A Framework for Embodied Semantics. Cerebral Cortex 26 (5):2018–2034. doi:10.1093/cercor/bhv020

Fox MD, Snyder AZ, Vincent JL, Corbetta M, Van Essen DC, Raichle ME (2005) The human brain is intrinsically organized into dynamic, anticorrelated functional networks. Proc Natl Acad Sci U S A 102 (27):9673–9678. doi:10.1073/pnas.0504136102

Graessner A, Zaccarella E, Hartwigsen G (2021) Differential contributions of left-hemispheric language regions to basic semantic composition. Brain Structure and Function 226 (2):501–518. doi:10.1007/s00429-020-02196-2

Graves WW, Boukrina O, Mattheiss SR, Alexander EJ, Baillet S (2017) Reversing the Standard Neural Signature of the Word-Nonword Distinction. J Cogn Neurosci 29 (1):79–94. doi:10.1162/jocn_a_01022

Handy TC (2000) Capacity Theory as a Model of Cortical Behavior. Journal of Cognitive Neuroscience 12 (6):1066–1069. doi:10.1162/08989290051137576

Humphreys GF, Hoffman P, Visser M, Binney RJ, Lambon Ralph MA (2015) Establishing task- and modality-dependent dissociations between the semantic and default mode networks. Proc Natl Acad Sci U S A 112 (25):7857–7862. doi:10.1073/pnas.1422760112

Humphreys GF, Lambon Ralph MA (2017) Mapping Domain-Selective and Counterpointed Domain-General Higher Cognitive Functions in the Lateral Parietal Cortex: Evidence from fMRI Comparisons of Difficulty-Varying Semantic Versus Visuo-Spatial Tasks, and Functional Connectivity Analyses. Cereb Cortex 27 (8):4199–4212. doi:10.1093/cercor/bhx107

Humphreys GF, Lambon Ralph MA, Simons JS (2021) A Unifying Account of Angular Gyrus Contributions to Episodic and Semantic Cognition. Trends Neurosci 44 (6):452–463. doi:10.1016/j.tins.2021.01.006

Humphries C, Binder JR, Medler DA, Liebenthal E (2006) Syntactic and Semantic Modulation of Neural Activity during Auditory Sentence Comprehension. Journal of Cognitive Neuroscience 18 (4):665–679. doi:10.1162/jocn.2006.18.4.665

Hung J, Wang X, Wang X, Bi Y (2020) Functional subdivisions in the anterior temporal lobes: a large scale meta-analytic investigation. Neurosci Biobehav Rev 115:134–145. doi:10.1016/j.neubiorev.2020.05.008

Huth AG, de Heer WA, Griffiths TL, Theunissen FE, Gallant JL (2016) Natural speech reveals the semantic maps that tile human cerebral cortex. Nature 532 (7600):453–458.

doi:10.1038/nature17637
Jackson RL, Cloutman LL, Lambon Ralph MA (2019) Exploring distinct default mode and semantic networks using a systematic ICA approach. Cortex 113:279–297. doi:10.1016/j.cortex.2018.12.019
Kuznetsova A, Brockhoff PB, Christensen RHB (2017) lmerTest Package: Tests in Linear Mixed Effects Models. Journal of Statistical Software 82 (13):1–26. doi:10.18637/jss.v082.i13
Lin N, Bi Y, Zhao Y, Luo C, Li X (2015) The theory-of-mind network in support of action verb comprehension: evidence from an fMRI study. Brain Lang 141:1–10. doi:10.1016/j.bandl.2014.11.004
Lin N, Wang X, Xu Y, Wang X, Hua H, Zhao Y, Li X (2018a) Fine Subdivisions of the Semantic Network Supporting Social and Sensory-Motor Semantic Processing. Cereb Cortex 28 (8):2699–2710. doi:10.1093/cercor/bhx148
Lin N, Xu Y, Wang X, Yang H, Du M, Hua H, Li X (2019) Coin, telephone, and handcuffs: Neural correlates of social knowledge of inanimate objects. Neuropsychologia 133:107187. doi:10.1016/j.neuropsychologia.2019.107187
Lin N, Xu Y, Yang H, Zhang G, Zhang M, Wang S, Hua H, Li X (2020) Dissociating the neural correlates of the sociality and plausibility effects in simple conceptual combination. Brain Struct Funct 225 (3):995–1008. doi:10.1007/s00429-020-02052-3
Lin N, Yang X, Li J, Wang S, Hua H, Ma Y, Li X (2018b) Neural correlates of three cognitive processes involved in theory of mind and discourse comprehension. Cogn Affect Behav Neurosci 18 (2):273–283. doi:10.3758/s13415-018-0568-6
Mar RA (20102011) The Neural Bases of Social Cognition and Story Comprehension. Annual Review of Psychology 62 (1):103–134. doi:10.1146/annurev-psych-120709-145406
Mattheiss SR, Levinson H, Graves WW (2018) Duality of Function: Activation for Meaningless Nonwords and Semantic Codes in the Same Brain Areas. Cereb Cortex 28 (7):2516–2524. doi:10.1093/cercor/bhy053
Meyer ML, Collier E (2020) Theory of minds: managing mental state inferences in working memory is associated with the dorsomedial subsystem of the default network and social integration. Soc Cogn Affect Neurosci 15 (1):63–73. doi:10.1093/scan/nsaa022
Meyer ML, Spunt RP, Berkman ET, Taylor SE, Lieberman MD (2012) Evidence for social working memory from a parametric functional MRI study. Proc Natl Acad Sci U S A 109 (6):1883–1888. doi:10.1073/pnas.1121077109
Meyer ML, Taylor SE, Lieberman MD (2015) Social working memory and its distinctive link to social cognitive ability: an fMRI study. Soc Cogn Affect Neurosci 10 (10):1338–1347. doi:10.1093/scan/nsv065
Pallier C, Devauchelle A-D, Dehaene S (2011) Cortical representation of the constituent structure of sentences. Proceedings of the National Academy of Sciences 108 (6):2522. doi:10.1073/pnas.1018711108
Price AR, Bonner MF, Peelle JE, Grossman M (2015) Converging Evidence for the Neuroanatomic Basis of Combinatorial Semantics in the Angular Gyrus. The Journal of Neuroscience 35 (7):3276. doi:10.1523/JNEUROSCI.3446-14.2015
Raichle ME, MacLeod AM, Snyder AZ, Powers WJ, Gusnard DA, Shulman GL (2001) A default mode of brain function. Proc Natl Acad Sci U S A 98 (2):676–682. doi:10.1073/pnas.98.2.676
Renoult L, Davidson PS, Palombo DJ, Moscovitch M, Levine B (2012) Personal semantics: at the

crossroads of semantic and episodic memory. Trends Cogn Sci 16 (11):550–558. doi:10.1016/j.tics.2012.09.003

Schurz M, Radua J, Tholen MG, Maliske L, Margulies DS, Mars RB, Sallet J, Kanske P (2021) Toward a hierarchical model of social cognition: A neuroimaging meta-analysis and integrative review of empathy and theory of mind. Psychological Bulletin 147 (3):293–327. doi:10.1037/bul0000303

Seghier ML (20122013) The Angular Gyrus: Multiple Functions and Multiple Subdivisions. The Neuroscientist 19 (1):43–61. doi:10.1177/1073858412440596

Seghier ML, Fagan E, Price CJ (2010) Functional Subdivisions in the Left Angular Gyrus Where the Semantic System Meets and Diverges from the Default Network. The Journal of Neuroscience 30 (50):16809. doi:10.1523/JNEUROSCI.3377-10.2010

Smallwood J, Bernhardt BC, Leech R, Bzdok D, Jefferies E, Margulies DS (2021) The default mode network in cognition: a topographical perspective. Nat Rev Neurosci 22 (8):503–513. doi:10.1038/s41583-021-00474-4

Tamir DI, Bricker AB, Dodell-Feder D, Mitchell JP (2016) Reading fiction and reading minds: the role of simulation in the default network. Soc Cogn Affect Neurosci 11 (2):215–224. doi:10.1093/scan/nsv114

Thornton MA, Mitchell JP (2018) Theories of Person Perception Predict Patterns of Neural Activity During Mentalizing. Cereb Cortex 28 (10):3505–3520. doi:10.1093/cercor/bhx216

Uddin LQ, Supekar K, Amin H, Rykhlevskaia E, Nguyen DA, Greicius MD, Menon V (2010) Dissociable Connectivity within Human Angular Gyrus and Intraparietal Sulcus: Evidence from Functional and Structural Connectivity. Cerebral Cortex 20 (11):2636–2646. doi:10.1093/cercor/bhq011

Wang X, Gao Z, Smallwood J, Jefferies E (2021) Both Default and Multiple-Demand Regions Represent Semantic Goal Information. J Neurosci 41 (16):3679–3691. doi:10.1523/jneurosci.1782-20.2021

Wilson-Mendenhall CD, Simmons WK, Martin A, Barsalou LW (2013) Contextual Processing of Abstract Concepts Reveals Neural Representations of Nonlinguistic Semantic Content. Journal of Cognitive Neuroscience 25 (6):920–935. doi:10.1162/jocn_a_00361

Xu J, Kemeny S, Park G, Frattali C, Braun A (2005) Language in context: emergent features of word, sentence, and narrative comprehension. Neuroimage 25 (3):1002–1015. doi:10.1016/j.neuroimage.2004.12.013

Yan CG, Wang XD, Zuo XN, Zang YF (2016) DPABI: Data Processing & Analysis for (Resting-State) Brain Imaging. Neuroinformatics 14 (3):339–351. doi:10.1007/s12021-016-9299-4

Yarkoni T, Barch DM, Gray JR, Conturo TE, Braver TS (2009) BOLD correlates of trial-by-trial reaction time variability in gray and white matter: a multi-study fMRI analysis. PLoS One 4 (1):e4257. doi:10.1371/journal.pone.0004257

Yeo BT, Krienen FM, Sepulcre J, Sabuncu MR, Lashkari D, Hollinshead M, Roffman JL, Smoller JW, Zöllei L, Polimeni JR, Fischl B, Liu H, Buckner RL (2011) The organization of the human cerebral cortex estimated by intrinsic functional connectivity. J Neurophysiol 106 (3):1125–1165. doi:10.1152/jn.00338.2011

Zahn R, Moll J, Krueger F, Huey ED, Garrido G, Grafman J (2007) Social concepts are represented in the superior anterior temporal cortex. Proc Natl Acad Sci U S A 104 (15):6430–6435. doi:10.1073/pnas.0607061104

Zhang G, Xu Y, Zhang M, Wang S, Lin N (2021) The brain network in support of social semantic accumulation. Soc Cogn Affect Neurosci 16 (4):393–405. doi:10.1093/scan/nsab003

Zwaan RA, Radvansky GA (1998) Situation models in language comprehension and memory. Psychol Bull 123 (2):162–185. doi:10.1037/0033-2909.123.2.162

Tables

Table 1. Variables that were manipulated or controlled in the high and low social-semantic-richness narrative stimuli

	Narrative-level variables						Sentence-level variables		Word-level variable	
	Social semantic richness	Semantic plausibility	Averaged plausibility across four sentences	Coherence	Number of words per narrative	Number of characters per narrative	Social semantic richness	Semantic plausibility	Number of characters per word	Log transferred word frequency
HS	5.86	6.45	6.78	6.71	28.97	48.81	4.90	6.78	1.65	2.05
	(0.42)	(0.26)	(0.11)	(0.29)	(1.06)	(1.20)	(0.95)	(0.20)	(0.06)	(0.14)
LS	1.36	6.41	6.72	6.74	28.81	48.41	1.39	6.76	1.66	2.05
	(0.27)	(0.40)	(0.17)	(0.23)	(1.40)	(1.37)	(0.30)	(0.48)	(0.07)	(0.14)

Note. The variables were presented in the form of mean (standard deviation). Condition labels: HS - high social-semantic richness narrative stimuli; LS - low-social-semantic-richness narrative stimuli.

Table 2. Overview of the five previous studies included in the ROI analysis.

Study	Number of participants	Tasks	Stimulus type	Example trial	
				High social semantic richness	Low social semantic richness
Lin et al. (2018a)	19	Semantic relatedness judgment	High-imageability verb	"Kiss – Embrace"	"Run – Walk"
			Low-imageability verb	"Adore – Admire"	"Remember – Forget"
Lin et al. (2019)	20	Semantic relatedness judgment	Object noun	"Textbook – Blackboard"	"Sheet – Pillow"
Lin et al. (2020)	20	Plausibility judgment	High-plausibility phrase	"To detain suspects"	"To sharpen a knife"
			Low-plausibility phrase	"To detain greeting cards"	"To sharpen cotton"
Zhang et al. (2021)	33	Silent reading	Narrative	"Liu Mei and her friends were going to Tiananmen Square. / Her friend planed to set out at 3 a.m. / Liu Mei said it did not have to be so early. / Finally they set out at 4:30 a.m."	"Li Jun opened the window of his room. / The cold wind flow into his room . / Li Jun felt cold. / So he closed the window."
			Unconnected sentences	"Liu Mei asked her sister for help. / The new roommate was kind and clean. / Liu Mei promised her customers discounts. / Liu Mei learned a lot about Chinese chess."	"Li Jun washed clothes at home. / These flowers made the house lively. / Li Jun found that the water pipe in the toilet was leaking. / Li Jun only picked the edible mushrooms."
			Wordlists	"Liu-Mei Receive College Together Chess Young / Teacher Walk Situation Tuitor	"Li-Jun Body Walk Eye Second Brain / Sleep Ant Onion Finding Take Cover /

				Admir Learn / Coquetry Liu-Mei Naughty Teach Visit Promise / Self Liu-Mei Teacher Refusion Go Plan”	Ji-Jun Bang Quick Pesticide Pipe / Sky Li-Jun Bang Force Stop Mushroom”
Lin et al. (2018b)	39	Reading comprehension	Narrative beginning	“Li Ming and Xiao Fang searched the house for their keys with no luck.”	“A volcano erupted on a Caribbean island three months ago.”
			Narrative ending	“Suddenly Li Ming noticed the keys behind the sofa.”	“Satellite photographs show the island as it was before the eruption.”

1

Table 3. Whole-brain analysis results of the main effects and interactions (voxel-wise $p < .001$, cluster-wise FWE $p < .05$)

Contrasts	Anatomical region of the peak voxel	Number of voxels	MNI coordinates of the peak voxel			Peak t value
			x	y	z	
Social semantic effect: (HSHL + HSLL) - (LSHL + LSLL)						
(HSHL + HSLL) > (LSHL + LSLL)						
	Left Middle Temporal Gyrus	1490	-54	-6	-15	13.488
	Left Posterior Cingulate Gyrus	636	0	-57	21	10.949
	Right Middle Temporal Gyrus	1011	51	3	-24	10.203
	Left Dorsal Medial Prefrontal Cortex	569	-12	48	42	7.177
	Left Ventral Medial Prefrontal Cortex	68	0	48	-15	7.093
(HSHL + HSLL) < (LSHL + LSLL)						
	Left Inferior Frontal Gyrus	51	-30	36	-9	6.603
	Right Middle Frontal Gyrus	66	45	39	9	5.950
	Left Inferior Frontal Cortex	69	-45	36	18	5.075
Difficulty effect: (HSHL + LSHL) - (HSLL + LSLL)						
(HSHL + LSHL) > (HSLL + LSLL)						
	Left Inferior Parietal lobe	2424	-42	-42	42	9.963
	Left Middle Frontal Gyrus	1928	-27	3	51	9.771
	Left Precentral Gyrus	660	-48	9	30	8.041
	Right Cerebellum lobe	96	30	-63	-30	7.663
	Left Cerebellum lobe	252	-24	-60	-30	6.436
	Left Inferior Frontal Gyrus	225	-39	45	6	5.369
	Right Insula	39	30	24	0	4.643
(HSHL + LSHL) < (HSLL + LSLL)						

Right Paracentral Lobe	302	12	-33	51	5.571
Right Supramarginal Gyrus	43	66	-42	24	5.071
Right Superior Occipital Gyrus	97	15	-93	18	4.969
Interaction: (HSHL - LSHL) - (HSLL - LSLL)					
(HSHL - LSHL) > (HSLL - LSLL)					
None					
(HSHL - LSHL) < (HSLL - LSLL)					
None					
Task effect: HSHL + LSHL + HSLL + LSLL					
(HSHL + LSHL + HSLL + LSLL) > 0					
Left fusiform cortex	8530	-42	-63	-15	19.656
Right middle frontal gyrus	1069	33	0	57	11.452
Right thalamus	283	18	-12	3	10.450
Right superior parietal lobe	382	36	-48	45	7.696
(HSHL + LSHL + HSLL + LSLL) < 0					
Middle cingular cortex	7007	0	-21	39	15.292
Right parahippocampal cortex	330	33	-39	-9	9.391
Left lingual gyrus	149	-27	-42	-3	8.554
Left insular cortex	159	-39	-18	-3	7.488
Right inferior frontal gyrus, triangular part	57	39	36	6	6.324

Condition labels: HSHL - high social semantic richness and high working memory load; HSLL - high social semantic richness and low working memory load; LSHL - low social semantic richness and high working memory load; LSLL - low social semantic richness and low working memory load.

Table 4. ROI analysis results

ROI	Contrast											
	Social semantic effect: HSHL + HSLL - LSHL - LSLL			Difficulty effect: HSHL - HSLL + LSHL - LSLL			Interaction: HSHL - HSLL - LSHL + LSLL			Task effect: HSHL + HSLL + LSHL + LSLL		
	beta (SE)	df	t	beta (SE)	df	t	beta (SE)	df	t	beta (SE)	df	t
ROIs of the social semantic network												
LATL	0.342	544	18.288^{***+}	-0.082	544	-4.356^{***+}	-0.028	544	-0.736	0.105	24.923	2.101*
	(0.019)			(0.019)			(0.037)			(0.050)		
RATL	0.335	544	15.432^{***+}	-0.110	544	-5.072^{***+}	-0.004	544	-0.100	0.072	24.791	1.081
	(0.022)			(0.022)			(0.043)			(0.066)		
LDMPFC	0.368	544	10.415^{***+}	-0.192	544	-5.425^{***+}	-0.087	544	-1.229	-0.200	23.950	-2.117*
	(0.035)			(0.035)			(0.071)			(0.094)		
LTPJ	0.375	544	11.083^{***+}	-0.133	544	-3.926^{***+}	-0.123	544	-1.818	-0.055	25.912	-0.518
	(0.034)			(0.034)			(0.068)			(0.107)		
RTPJ	0.323	544	10.130^{***+}	-0.063	544	-1.973*	-0.081	544	-1.273	-0.102	26.225	-1.140
	(0.032)			(0.032)			(0.064)			(0.089)		
PC	0.411	544	12.952^{***+}	-0.107	544	-3.365^{***+}	-0.108	544	-1.702	-0.433	24.729	-5.942^{***+}
	(0.032)			(0.032)			(0.063)			(0.073)		
ROIs of the bilateral AG												
Left dorsal AG	-0.014	544	-0.488	0.368	544	12.449^{***+}	0.068	544	1.154	0.467	26.420	5.084^{***+}
	(0.030)			(0.030)			(0.059)			(0.092)		
Right dorsal AG	-0.013	544	-0.435	0.319	544	10.498^{***+}	0.076	544	1.249	0.315	23.998	3.919^{**+}
	(0.030)			(0.030)			(0.061)			(0.080)		
Left ventral AG	0.209	544	7.796^{***+}	0.051	544	1.913	-0.046	544	-0.852	-0.013	25.294	-0.155
	(0.027)			(0.027)			(0.054)			(0.082)		

Right ventral AG	0.133 (0.023)	544	5.802***+	0.007 (0.023)	544	0.327	-0.037 (0.046)	544	-0.803	-0.074 (0.063)	25.289	-1.175
Three subnetworks within the DMN												
DMN core	0.146 (0.022)	544	6.758***+	-0.033 (0.022)	544	-1.519	-0.069 (0.043)	544	-1.609	-0.312 (0.054)	21.161	-5.809***+
DMN DMPFC	0.175 (0.020)	544	8.685***+	-0.042 (0.020)	544	-2.094*	-0.055 (0.040)	544	-1.362	0.024 (0.056)	25.364	0.421
DMN MTL	0.060 (0.020)	544	2.953**+	-0.031 (0.020)	544	-1.527	-0.087 (0.041)	544	-2.132*	-0.268 (0.053)	18.996	-5.090***+

Note. *P < 0.05; **P < 0.01; ***P < 0.001.+ *t*-values surviving the Bonferroni correction in which the significance level is divided by the number of ROIs (for ROIs of the social semantic network, N=6; for ROIs of the bilaterial AG, N = 4; for the three subnetworks within DMN, N = 3). Condition labels: HSHL - high social semantic richness and high working memory load; HSLL - high social semantic richness and low working memory load; LSHL - low social semantic richness and high working memory load; LSLL - low social semantic richness and low working memory load. ROI labels: LATL, left anterior temporal lobe; RATL, right anterior temporal lobe; LDMPFC, left dorsal medial prefrontal cortex; LTPJ, left temporoparietal junction; RTPJ, right temporoparietal junction; PC, posterior cingulate; AG, angular gyrus; DMN core, the core subnetwork of the default mode network; DMN DMPFC, the dorsal medial prefrontal cortex subnetwork of the default mode network; DMN MTL, the medial temporal lobe subnetwork of the default mode network.

Figures

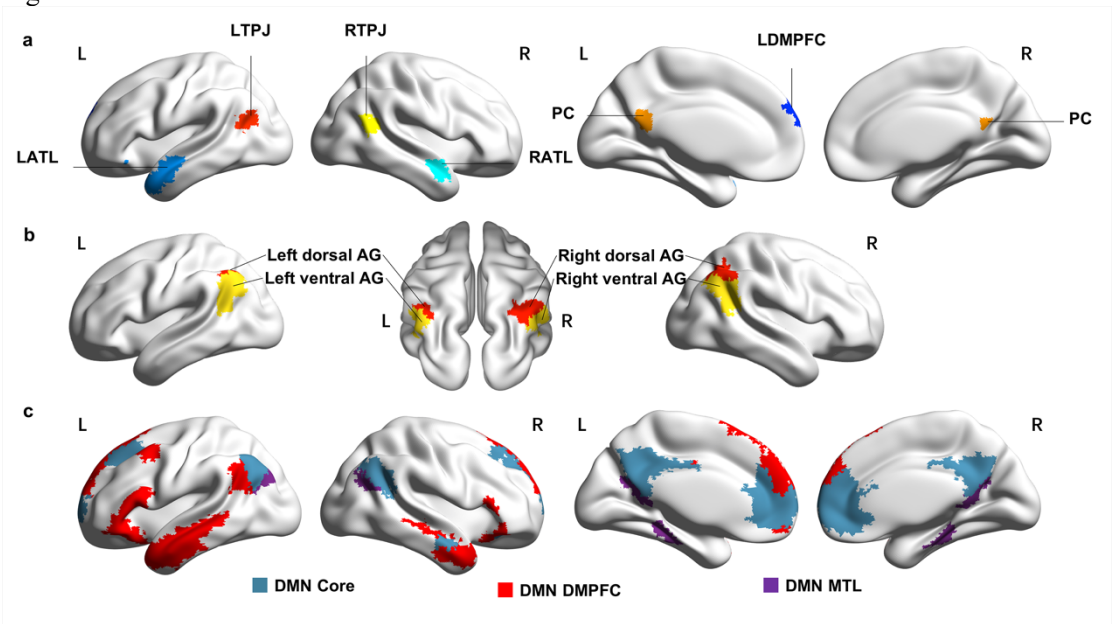

Fig. 1. ROIs used in our study. **a** ROIs of the social semantic network identified by Lin et al. (2019) using a word comprehension task. **b** ROIs of the Neurosynth-based functional subdivisions of the bilateral AG (2-cluster parcellation). **c** ROIs of the three resting-state subnetworks of the DMN (Yeo et al., 2011). ROI, region of interest; AG, angular gyrus; DMN, default mode network.

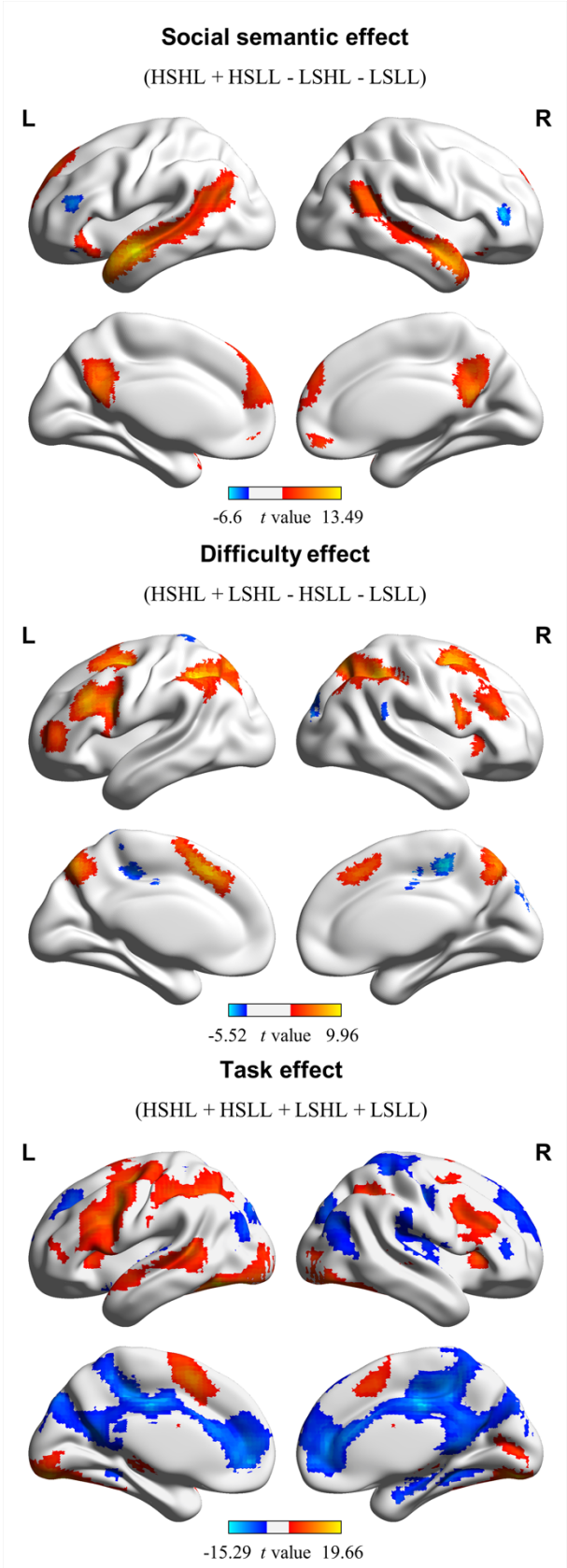

Fig. 2. Whole-brain analysis results. Condition labels: HSHL, high social semantic richness and high working memory load; HSLL, high social semantic richness and low working memory load; LSHL, low social semantic richness and high working memory load; LSLL, low social semantic richness and low working memory load.

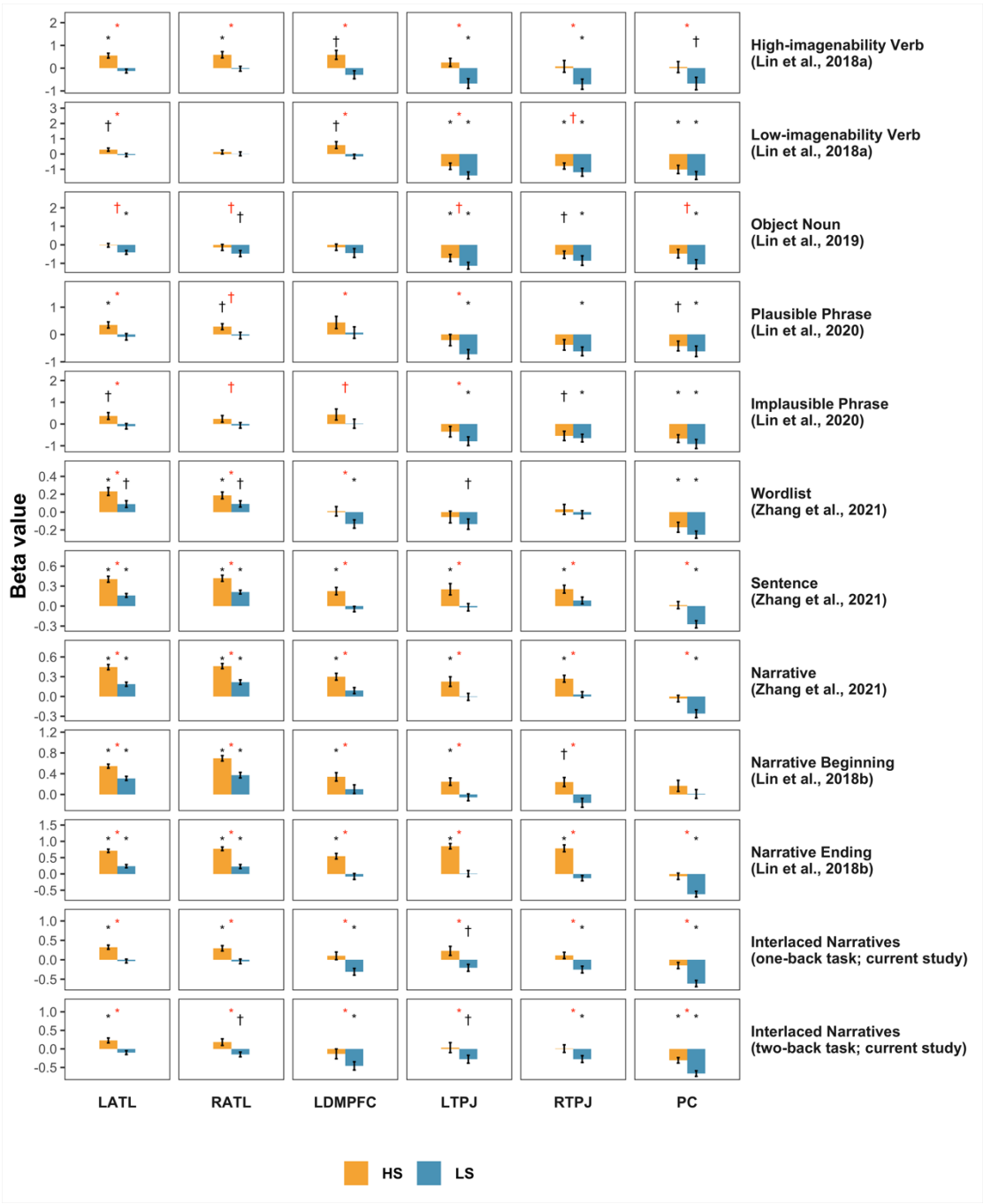

Fig. 3. Social semantic effects and task effects of the ROIs of the social semantic network in this and five previous studies using different types of stimuli and tasks. Condition labels: HS, high social semantic richness; LS, low social semantic richness. ROI: region of interest. ROI labels: LATL, left anterior temporal lobe; RATL, right anterior temporal lobe; LDMPFC, left dorsal medial prefrontal cortex; LTPJ, left temporoparietal junction; RTPJ, right temporoparietal junction; PC, posterior cingulate. The significance of the single-condition effects (HS or LS, black labels) and the social effects (HS to LS, red labels) was labeled in each subplot. $^{\dagger}p < .05$ but the *t*-values did not survive the Bonferroni correction in which the significance level was divided by the number of ROIs (N = 6). $^{*}p < .05$ and the *t*-values survived the Bonferroni correction.

Supplementary materials

Supplementary tables

Table S1. Four versions of structures in which the sentences were arranged in a block. Each experimental condition contained two blocks for each version of the structures. A and B represent two narratives, and the numbers following A or B represent the order of the sentences within the narrative.

	version 1	version 2	version 3	version 4
sentence 1	A1	A1	A1	A1
sentence 2	B1	B1	B1	B1
sentence 3	A2	A2	B2	B2
sentence 4	B2	A3	A2	B3
sentence 5	B3	B2	B3	A2
sentence 6	B4	B3	A3	B4
sentence 7	A3	A4	A4	A3
sentence 8	A4	B4	B4	A4

Note. Each experimental condition contained two blocks of each version of structures. A and B represents two stories and the numbers following A or B represents the order of the sentence within the story.

Table S2. Coherence rating scores of the paired sentences to be decided in the fMRI task

	Conditions	Coherence rating scores
Within-narrative sentence pairs	HSHL	6.18 (0.61)
	HSLL	6.23 (0.56)
	LSHL	6.09 (0.51)
	LSLL	6.32 (0.51)
Between-narrative sentence pairs	HSHL	1.30 (0.35)
	HSLL	1.20 (0.32)
	LSHL	1.21 (0.30)
	LSLL	1.20 (0.32)

Note. The coherence rating scores were presented in the form of mean (standard deviation). Condition labels: HSHL - high social semantic richness and high working memory load; HSLL - high social semantic richness and low working memory load; LSHL - low social semantic richness and high working memory load; LSLL - low social semantic richness and low working memory load.

Table S3. Mean (SD) accuracy and reaction time in the second preliminary behavioral experiment

Conditions	Accuracy	Reaction time
HSHL	91.0% (4.0%)	2689 (1263)
HSLL	96.9% (8.1%)	1850 (926)
LSHL	91.6% (8.1%)	2663 (1330)
LSLL	96.1% (3.4%)	1707 (827)

Note. Condition labels: HSHL - high social semantic richness and high working memory load; HSLL - high social semantic richness and low working memory load; LSHL - low social semantic richness and high working memory load; LSLL - low social semantic richness and low working memory load.

Table S4. Supplementary ROI analysis results

ROI	Contrast											
	Social semantic effect: HSHL + HSLL - LSHL - LSLL			Difficulty effect: HSHL - HSLL + LSHL - LSLL			Interaction: HSHL - HSLL - LSHL + LSLL			Task effect: HSHL + HSLL + LSHL + LSLL		
	beta	SE	t	beta	SE	t	beta	SE	t	beta	SE	t
Social semantic network defined using the Neurosynth database	0.285	0.021	13.64***	-0.081	0.021	-3.86***	-0.078	0.042	-1.867	0.021	0.06	0.349
Left AG c1	-0.026	0.03	-0.893	0.457	0.03	15.45^{***+}	0.014	0.059	0.244	0.684	0.095	7.198^{***+}
Right AG c1	-0.006	0.033	-0.172	0.409	0.033	12.226^{***+}	0.05	0.067	0.742	0.513	0.1	5.149^{***+}
Left AG c2	0.003	0.028	0.122	0.272	0.028	9.753^{***+}	0.07	0.056	1.262	0.265	0.077	3.433^{**+}
Right AG c2	-0.008	0.027	-0.288	0.19	0.027	7.157^{***+}	0.065	0.053	1.226	0.077	0.066	1.16
Left AG c3	0.223	0.035	6.454^{***+}	0.116	0.035	3.346^{**+}	-0.031	0.069	-0.446	-0.135	0.107	-1.259
Right AG c3	0.117	0.028	4.139^{***+}	0.066	0.028	2.348*	-0.049	0.056	-0.869	-0.174	0.073	-2.392*
Left AG c4	0.275	0.027	10.265^{***+}	-0.052	0.027	-1.936	-0.103	0.054	-1.923	0.075	0.087	0.862
Right AG c4	0.213	0.025	8.592^{***+}	-0.075	0.025	-3.045^{**+}	-0.059	0.05	-1.186	-0.03	0.071	-0.422

Note. $^{*}P < 0.05$; $^{**}P < 0.01$; $^{***}P < 0.001$. $^{+}$ *t*-values surviving the Bonferroni correction in which the significance level is divided by the number of ROIs within AG (N = 8). Condition labels: HSHL - high social semantic richness and high working memory load; HSLL - high social semantic richness and low working memory load; LSHL - low social semantic richness and high working memory load; LSLL - low social semantic richness and low working memory load. ROI labels: AG, angular gyrus

Supplementary figures

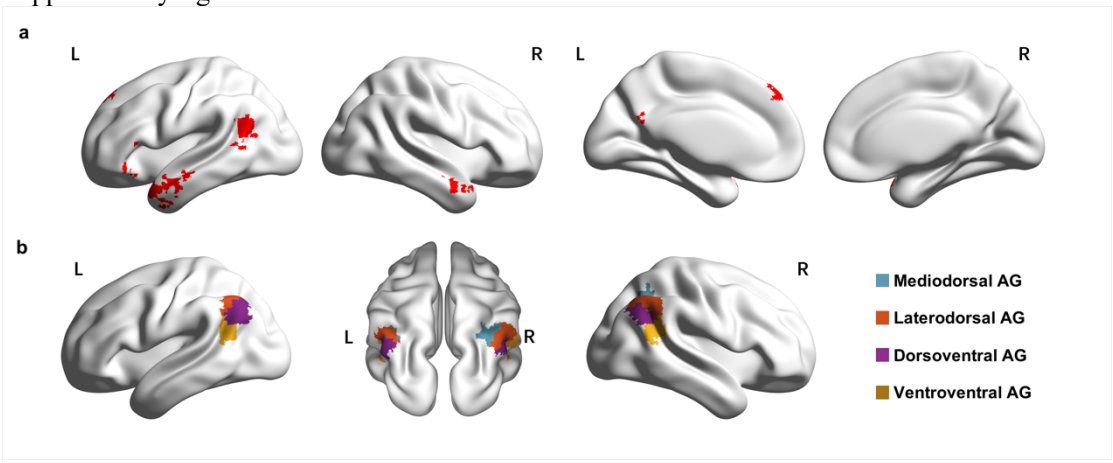

Fig. S1. Supplementary ROIs used in the study. **a** ROI of the social semantic network based on the Neurosynth database (Zhang et al., 2021). **b** ROIs of the Neurosynth-based functional subdivisions of the bilateral AG (4-cluster parcellation).

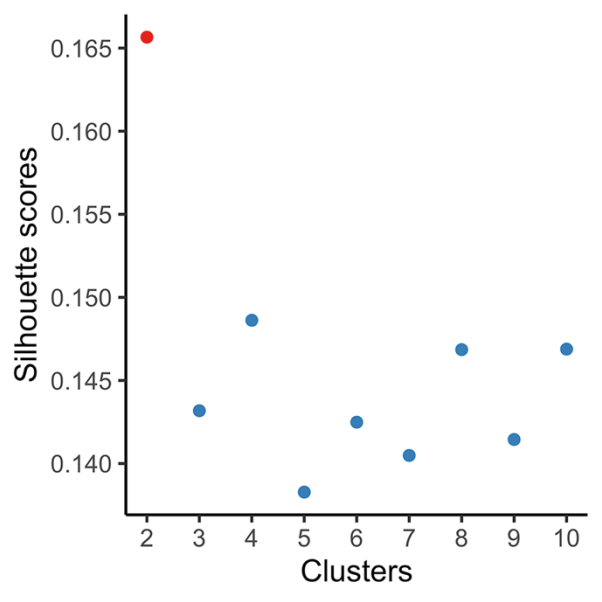

Fig. S2. Silhouette scores for the clusters from k = 1 to 10 for the AG ROI mask, in which k = 2 (red dots) had the best performance.

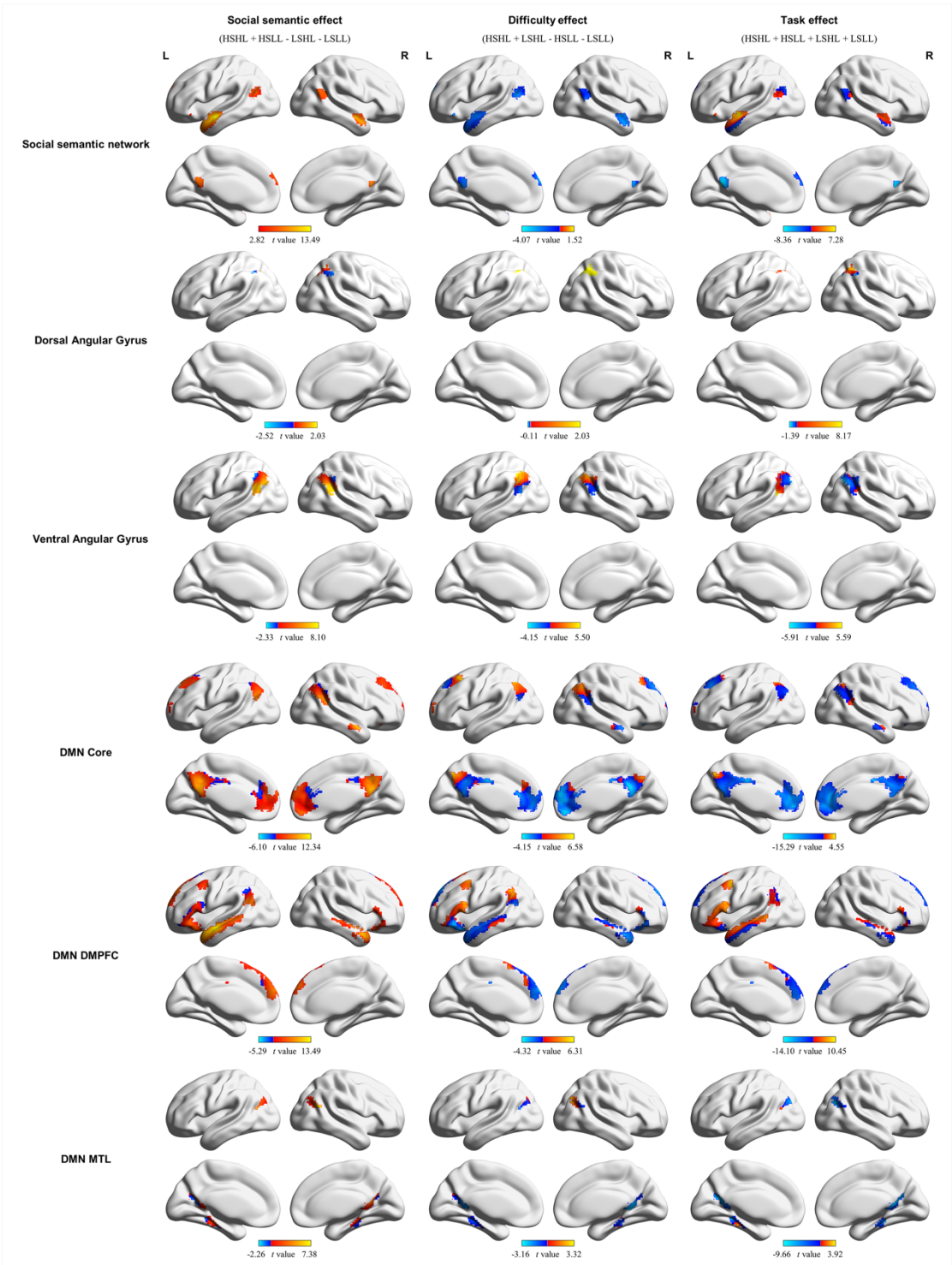

Fig. S3. Inspection of the within-ROI spatial functional homogeneity as reflected by the voxel-wise activation results. The supplementary ROIs are not shown. Condition labels: HSHL, high social semantic richness and high working memory load; HSLL, high social semantic richness and low working memory load; LSHL, low social semantic richness and high working memory load; LSLL, low social semantic richness and low working memory load. ROI labels: DMN core, core subnetwork of the default mode network; DMN DMPFC, dorsal medial prefrontal cortex subnetwork of the default mode network; DMN MTL, medial temporal lobe subnetwork of the default mode network.

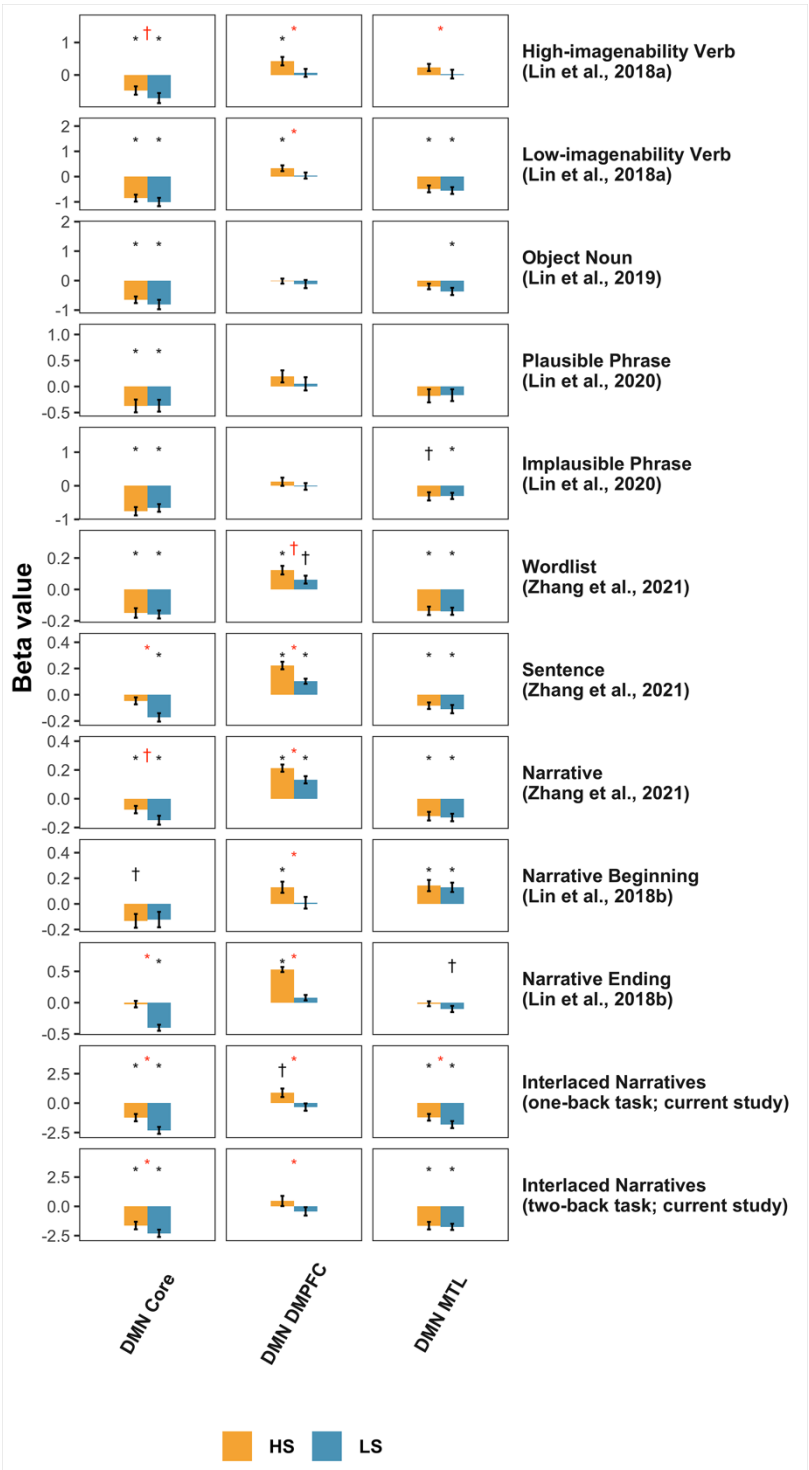

Fig. S4. Social semantic effects and task effects of the three subnetworks of the DMN in the study and five previous experiments using different types of stimuli and tasks. Condition labels: HS, high social semantic richness; LS, low social semantic richness. ROI labels: DMN core, core subnetwork of the DMN; DMN DMPFC, dorsal medial prefrontal cortex subnetwork of the DMN; DMN MTL, medial temporal lobe subnetwork of the DMN. The significance of the single-condition effects (HS or LS, black labels) and the social effects (HS to LS, red labels) was labeled in each subplot. $^{\dagger}p < .05$ but the *t*-values did not survive the Bonferroni correction in which the significance level was divided by the number of ROIs (N = 3). $^{*}p < .05$ and the *t*-values survived the Bonferroni correction.